Multiconfiguration Dirac-Fock calculations in open-shell atoms: Convergence methods and satellite spectra of the copper $K\alpha$ photoemission spectrum

C. T. Chantler[*] and J. A. Lowe

School of Physics, University of Melbourne, Victoria 3101, Australia

I. P. Grant

Mathematical Institute, Oxford University, Oxford, United Kingdom
(Received 18 August 2010; published 8 November 2010)

The copper $K\alpha$ photoemission spectra is one of the most widely studied. Recent Dirac-Fock calculations have produced transition energies in good agreement with experiment, though they have relied on approximations that may not be transferable to other complex atoms in which uncertainties in theoretical results are dominated by poor convergence. Through a detailed examination of convergence issues in the copper spectrum, we consider the accuracy obtainable with the multiconfiguration Dirac-Fock (MCDF) method, provide the first determination of fine structure contributions to the spectrum, and demonstrate reliable techniques for modeling spectator states with vacancies in the $3p$, $3d$, and $4s$ shells.

I. INTRODUCTION

Plasma physics and astrophysics often interrogate spectra from ionized species and species with open shells [1]. In astrophysics, transition-metal x-ray spectra are commonly used as diagnostics for black holes, neutron stars, and other galactic phenomena [2], and the many-multiplet method used to identify temporal variations of the fine structure constant depends on transition-metal atomic-structure calculations [3]. Contaminants in fusion and tokamak research are commonly transition-metal plasmas affecting performance [4], while similar species in fission reactor technology can be important in activation and lifetime estimates and hence in contaminant radiation issues [5]. Characteristic radiation is used as a diagnostic for laser-produced fast-ignition fusion [6] and in the study of electron propagation near intense laser spots [7]. There is also a need for improved understanding of the x-ray spectra used in mammography in order to improve precision [8].

The structure of the photoemission lines of the transition metals has been the subject of numerous investigations [9–12]. The $K\alpha$ line is the most intense x-ray emission and refers to the transition $1s^{-1} \rightarrow 2p^{-1}$ (the notation $1s^{-1}$ refers to a vacancy in the $1s$ shell). Separate peaks resulting from transitions to $2p_{\frac{3}{2}}^{-1}$ and $2p_{\frac{1}{2}}^{-1}$ are labeled $K\alpha_1$ and $K\alpha_2$.

The asymmetric $K\alpha$ line shapes and satellite features observed experimentally are indicative of processes other than a single ionization event followed by a bound-bound transition. Of the various explanations put forth to explain the $K\alpha$ line shape [10,13,14], the shake-off mechanism, in which a second electron is ionized as well as the core electron, appears to be the major contributor [15,16]. The relativistic multiconfiguration Dirac-Fock (MCDF) method has been highly successful in relatively simple atoms since the 1960s and 1970s, especially for low-Z or highly ionized atoms, e.g., in [17,18]. Conversely, very few studies of open-shell or highly excited atoms exist, despite their wide application. There are several reasons for this, including rapid growth of computation time, failure of

convergence, and multiple near-degenerate eigenstates—the problems are qualitatively and quantitatively different from the closed-shell case.

II. CALCULATION

The MCDF method has been described widely [19]. Atomic states are expanded into linear combinations of configuration state functions (CSFs) of well-defined parity and angular momentum,

$$\Psi(\Pi J M) = \sum_r c_r \Phi(\gamma_r \Pi J M), \qquad (1)$$

where Φ_r are a set of Slater-determinant CSFs forming an (incomplete) orthonormal basis and γ_r contains all the quantum numbers necessary to distinguish states. The mixing coefficients, c_r, are determined by diagonalization of the Dirac Hamiltonian, which occurs simultaneously with the optimization of the radial wave functions. In the MCDF implementation used herein QED and finite nuclear mass effects are added perturbatively.

The standard approach is to use the (restricted) active space method. A single or minimal set of reference CSF(s) serve as a zeroth order basis, and higher-order corrections are included by increasing the size of the CSF basis. The reference CSF is often divided into the core and an active set of valence shells, and the basis set is expanded by allowing single or multiple excitations within the active set. Through systematic enlargement of the active set, convergence can be monitored.

As the number of electrons and the number of active shells increases, the size of the CSF basis increases rapidly. Usually only single and double excitations from the reference configuration are considered; however, the number of CSFs in open-shell atoms still quickly escalates beyond practical limits—expansion of the ground state of calcium to the $n = 6$ layer requires ∼5,000 CSFs, scandium requires ∼275,000, and titanium requires ∼2,000,000. An ionized transition metal with a spectator vacancy can have three or four open shells, leading to CSF bases orders of magnitude larger again and with thousands of near-degenerate energy eigenstates [20]. Copper,

---

*chantler@unimelb.edu.au

with a full $3d$ shell and a single unpaired $4s$ electron, provides a useful starting point for investigations into open-shell atoms.

Deutsch's early investigation [9] associated the asymmetry of the copper $K\alpha$ lines with a population of initial states containing an additional vacancy in the $3d$ shell ("spectator" states). Deutsch's MCDF calculations allowed the identification of separate diagram and spectator contributions; however, the use of a single-basis set for upper and lower states produced results that required an experimental-theoretical energy shift before agreement with experiment was achieved. Moreover, the removal of the $4s$ electron from the calculations essentially reduced the problem to a closed-shell case.

Recent work by Chantler *et al.* [15] has taken into consideration the $4s$ shell electron and produced results with a level of accuracy that surpasses those previously reported. This work challenges claims that the MCDF method is accurate to no more than 1–2 eV, with results accurate to < 0.1 eV for the $K\alpha$ lines. This level of accuracy allows theoretical results to be fit to experimental data without the need for the theoretical-experimental energy shift common to works of this nature in the past.

The increased level of accuracy achieved by Chantler *et al.* arises from the implementation of theoretical work by Olsen [21] in the GRASP2K code of Jönsson *et al.* [22], also used in the present work. This allows for the transformation of two nonorthogonal, incomplete basis sets (CSFs) into a single biorthogonal set, thus allowing for transition matrix elements to be calculated between them. It is well-known that relaxation of orbitals between initial and final states is an important contribution to matrix elements, and biorthogonalization allows this to be properly taken into account.

Despite the accuracy of these results, several approximations were made. Valence-valence configuration interactions involving the $4s$-shell electron were only included approximately, and the potentially significant multiplet splitting of the diagram lines was not calculated; rather, only the $J = 1$ to $J = 1$ transition was calculated, and statistical arguments were used to adjust the transition rates.

This previous calculation disposes of the core/valence distinction and allows substitutions from all shells while prohibiting excitations from lower shells into the open $4s$ shell. While this evidently provides excellent convergence when the active set includes the $n = 4$ layer, if the method is robust it must remain converged when the active set is expanded further. Moreover, if we wish to apply these methods to a range of complex atoms, such approximations will not always be sensible.

III. RESULTS AND DISCUSSION

In the present work we consider several models for generating the expanded set of CSFs. In method 1 we divide the reference configuration into a set of core orbitals ($1s$, $2s$, and $2p$) and an active set ($3s$, $3p$, $3d$, and $4s$). Valence-valence correlations are included by allowing single and double excitations within the active set of orbitals, which is expanded at each stage of the calculation. At this stage no core-valence correlations are considered. We employ the frozen-core approximation, wherein after each expansion of the active set the existing optimized orbitals are "frozen," and only the newly added orbitals are optimized. The $4s$ electron was included in the calculation of the $n = 3$ layer before it was frozen, and the active set was expanded to the $n = 5$ layer.

In method 2 we take into account core-valence correlations by allowing excitations from the core to the $n = 4$ layer, with the restriction that no more than a single electron is excited from the core. In method 3 we extend the core-valence correlations by allowing both single and double excitations from the $n = 2$ layer and allow core excitations into the $n = 5$ layer.

In method 4 we dispense with the core or active set approach entirely and allow single and double excitations from all shells with the restriction that no excitations into the $4s$ shell are allowed. Since double excitations from the $n = 1$ to $n = 4,5$ layers are of order 300 eV, we do not expect them to significantly alter the results. We find, however, that inclusion of these CSFs drastically alters the transition energies and reduces agreement between the gauges, producing results at the $n = 5$ level that are in poor agreement with experiment. The inclusion of CSFs with a hollow core shell introduces convergence difficulties, as correlation orbitals of the same symmetry tend to collapse to unphysically small radii. Despite the small

TABLE I. Convergence of Cu $K\alpha$ diagram energies and length/velocity gauge transition strengths. Method 1: Valence-valence correlations only. Method 2: Core-valence correlations to the $n = 4$ level. Method 3: Core-valence correlations to the $n = 5$ level. Method 4: All possible excitations. Method 4 clearly leads to false results. Absolute transition energies vary with the basis set; however, the energy spacing and relative intensities calculated with methods 1–3 are in excellent agreement with one another. The ratio of oscillator strengths is a good indicator of convergence.

Active Set	Method 1		Method 2		Method 3		Method 4	
	Energy (eV)	A^L/A^V	Energy (eV)	A^L/A^V	Energy (eV)	A^L/A^V	Energy (eV)	A^L/A^V
$2p_{1/2} \rightarrow 1s$								
No Correlation	8030.79	0.99245	8030.79	0.99245	8030.79	0.99245	8030.79	0.99245
Correlation to $n = 4$	8027.87	0.99303	8027.95	1.00004	8027.91	1.00033	8027.91	1.00033
Correlation to $n = 5$	8027.90	0.99300	8027.98	0.99971	8027.90	0.99301	8029.90	1.0173
$2p_{3/2} \rightarrow 1s$								
No Correlation	8050.82	0.99263	8050.82	0.99263	8050.82	0.99263	8050.82	0.99263
Correlation to $n = 4$	8047.80	0.99329	8047.88	1.00005	8047.84	1.00042	8047.84	1.00042
Correlation to $n = 5$	8047.85	0.99324	8047.93	0.99999	8047.85	0.99325	8046.87	1.01697
Spacing	19.95		19.95		19.95		16.97	
Relative Intensities	0.510		0.510		0.512		0.354	

contribution of these CSFs to the eigenstates of interest, this poor convergence appears to have a significant effect. The results of these four methods are presented in Table I.

It is generally accepted that if wave functions are converging, a ratio of transition strengths calculated in the length and velocity gauges that approaches unity boosts confidence in the accuracy of the results. In all four methods the ratio of transition strengths in length and velocity gauges is closest to 1 after optimization of the $n = 4$ layer, and it is only with method 2 that we retain a high degree of convergence upon addition of the $n = 5$ layer.

Considering all four methods together, all calculated transition energies with oscillator ratios close to $1(|A^L - A^V|/A^L < 0.005)$ agree to within 0.08 eV. Moreover, the relative intensities and energy difference of the $K\alpha$ lines is robust, indicating that core-valence correlations are only significant for the $1s^{-1}$ state.

While absolute transition energies vary with the inclusion of core-valence correlations by up to 0.08 eV, the $K\alpha_1$, $K\alpha_2$ energy difference and relative intensities remain consistent to < 0.01 eV and 0.002, respectively; hence the structural features of the $K\alpha$ transition can be accurately calculated by considering only valence-valence correlations. This is true not only for the diagram lines presented above, but also for more extensive calculations for multiplet contributions and satellite lines.

This fact is vital for extension of the work to include more complex situations, as false or poor convergence becomes an otherwise insurmountable difficulty and an increasing CSF basis size increases computation time beyond practical limits. Relatively simple calculations can be used to determine structural features and the relative positions of lines, while detailed calculations are necessary only to scale the whole calculated spectrum.

To this end we adopted a new approach to the calculation of multiline transitions. In the first stage one or a few of the lines are calculated to a high degree of accuracy. Since calculations using large CSF bases are more prone to false convergences and unphysical answers (but are ultimately the most accurate), this stage proves to be highly difficult, and sometimes several lines must be tried before satisfactory convergence is obtained. Failure of wave functions to converge is a well-known and poorly understood problem in relativistic atomic structure calculations [23,24]. In the second stage we calculate all lines simultaneously with a smaller set of CSFs and scale
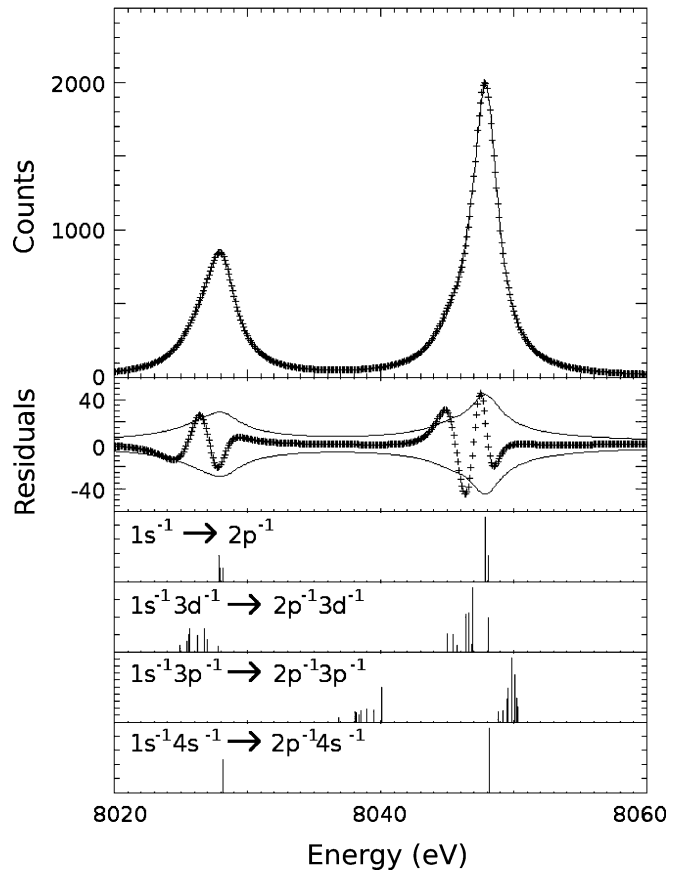

FIG. 1. Experimental and fitted theoretical spectrum for copper $K\alpha$. The curve bounding the residuals is $\pm\sigma$. The positions of the stick diagrams represent the transition energies contributing to the spectrum, and the height represents the intensity, normalized to the most intense transition of the group. The energy of the $4s$ spectator transition clearly indicates why approximate treatment of the open shell has provided good results in previous work.

the transition energies to agree with the results from stage one. The results of this method on the multiplet calculation are presented in Table II.

The $K\alpha$ spectator states have been calculated using this method. Transition energies were calculated for both the diagram and spectator states, taking into account only valence-valence correlations. The whole spectrum was then scaled so that the diagram lines matched the most accurate results presented in Table I as measured according to the oscillator ratios (method 2, $n = 4$). To correct for the divergence problem (closely spaced energy levels of the same J, Π diverge in energy due to the finite number of basis states) we used a weighted average.

The fit of our results to experimental data is presented in Fig. 1. The experimental data is a parametrization of Deutsch's experimental results [9]. Diagram and satellite intensities are fitted independently, and an additional three parameters characterize the transition widths—one each for $K\alpha_1$ and $K\alpha_2$ and one for the difference between diagram and spectator. The residuals remain almost entirely contained within $\pm\sigma$.

Figure 1 also includes stick diagrams illustrating the strengths and energies of the transitions contributing to the diagram and spectator spectra. As well as the dominant $3d$

TABLE II. Energies and Einstein A coefficients for copper $K\alpha_{1,2}$ spectrum fine structure as calculated using method 2. The $K\alpha_1$ and $K\alpha_2$ centroids (calculated using the weighted energies above) are 0.05 eV higher than predicted by the $J = 1 \rightarrow J = 1$ transition alone.

Transition	Energy (eV)	Strength ($A/10^{14}s^{-1}$)
$K\alpha_2$		
$J = 0 \rightarrow J = 1$	8028.18	3.08800
$J = 1 \rightarrow J = 0$	8027.95	1.02628
$J = 1 \rightarrow J = 1$	8027.95	2.04981
$K\alpha_1$		
$J = 0 \rightarrow J = 1$	8048.09	6.01073
$J = 1 \rightarrow J = 1$	8047.88	1.00575
$J = 1 \rightarrow J = 2$	8047.88	4.96683

TABLE III. Fitted parameters and standard deviations for the $K\alpha$ spectrum. The errors represent only the diagonal elements in the covariance matrix and do not consider the effect of the $\sim$0.1eV uncertainty in transition energies.

Parameter widths (eV)	Fit	Literature			
		[15]	[9]	[26]	
$2p_{\frac{3}{2}}$	2.72(8)	2.55(11)	2.68	1.81(5)	2.07 [27]
$2p_{\frac{1}{2}}$	2.20(4)	1.87(10)	2.08	2.93(7)	2.96 [27]
$2p_{\frac{3}{2}}3d$	3.61(29)	3.86(24)	2.75	1.21(15)	
$2p_{\frac{1}{2}}3d$	3.13(25)	3.18(25)	2.75	1.09(15)	
% pop.					
Diagram	74(1)	71(2.5)	69	72(3)	
Satellite	26(1)	29(2.5)	31	28(3)	23 [28]

spectator, we have calculated transition data for the $4s$ spectator and $3p$ spectator states. Deutsch presented his experimental results as a parametrization, and the $3p$ spectator (which would appear on the high-energy side of the $K\alpha_1$ peak) was not significant enough to be included in their parametrization.

Removal of the $4s$ electron has a minor effect on the spectrum. The transition energies are greater than the $J = 1 \rightarrow J = 1$ diagram case energies but less than the $J = 0 \rightarrow J = 1$ diagram case energies. This explains why both Deutsch and Chantler were able to obtain such excellent results despite incomplete treatments and why atomic calculations provide results that agree with solid-state experiments—solid-state

effects involving the $4s$ electron have little impact on the inner-shell transition energies.

Fitting parameters are presented in Table III. Despite using the same experimental data, our transition widths and spectator populations differ from Chantler *et al.*'s [15] and Deutsch's [9] due to the sensitivity of these parameters to the position of the satellite lines.

The fitted satellite population contributions are much greater than prevailing theoretical calculations predict. Kochur [12] and Mukoyama [25] predict $3d$ spectator populations of 14.5% and 10.3%, respectively, compared with the 26% found herein. However, all experimental determinations have so far shown this significant discrepancy [9,15,26,28], suggesting incomplete theoretical treatment of the shake-off process.

IV. CONCLUSION

We have shown that a complete MCDF treatment of highly excited open-shell atoms is possible and can yield results with an accuracy of < 0.1 eV. Our calculations of the $K\alpha$ transitions in copper agree well with experimental data. However, as previously observed, spectator intensities are greater than predicted theoretically. In principle, accurate data should be obtainable for the rest of the transition metals using these methods; however, our experience with copper suggests that problems encountered even within the transition-metal group are likely to be unique to each element and nontrivial to overcome.

[1] J. Cottam, F. Paerels, and M. Mendez, Nature **420**, 51 (2002).

[2] A. C. Fabian *et al.*, Nature **459**, 540 (2009).

[3] V. A. Dzuba, V. V. Flambaum, M. G. Kozlov, and M. Marchenko, Phys. Rev. A **66**, 022501 (2002).

[4] J. Gasparro, M. Hult, G. Bonheure, and P. Johnston, Applied Radiation and Isotopes **64**, 1130 (2006).

[5] P. Warwick and I. Croudace, Anal. Chim. Acta **567**, 277 (2006).

[6] L. Hudson and J. Seely, Radiat. Phys. Chem. **79**, 132 (2010).

[7] J. F. Seely, C. I. Szabo, P. Audebert, E. Brambrink, E. Tabakhoff, G. E. Holland, L. T. Hudson, A. Henins, P. Indelicato, and A. Gumberidze, High Energy Density Physics **5**, 263 (2009).

[8] C. T. Chantler, R. D. Deslattes, A. Henins, and L. Hudson, Brit. J. Radiol. **69**, 636 (1996).

[9] M. Deutsch, G. Hölzer, J. Härtwig, J. Wolf, M. Fritsch, and E. Förster, Phys. Rev. A **51**, 283 (1995).

[10] J. Finster, G. Leonhardt, and A. Meisel, J. Phys. (Paris) **32**, C4-218 (1971).

[11] R. Deslattes, E. Kessler, P. Indelicato, L. de Billy, E. Lindroth, and J. Anton, Rev. Mod. Phys. **75**, 35 (2003).

[12] A. G. Kochur, A. I. Dudenko, and D. Petrini, J. Phys. B **35**, 395 (2002).

[13] S. Doniach and M. Šunjić, J. Phys. C **3**, 285 (1970).

[14] L. Parratt, Phys. Rev. **49**, 502 (1936).

[15] C. T. Chantler, A. C. L. Hayward, and I. P. Grant, Phys. Rev. Lett. **103**, 123002 (2009).

[16] J. A. Lowe and C. T. Chantler, Phys. Lett. A **374**, 4756 (2010).

[17] S. Hasegawa, E. Recami, F. Yoshida, L. Matsuoka, F. Koike, S. Fritzsche, S. Obara, Y. Azuma, and T. Nagata, Phys. Rev. Lett. **97**, 023001 (2006).

[18] A. Natarajan and L. Natarajan, J. Phys. B **37**, 4789 (2004).

[19] I. Grant, *Relativistic Quantum Theory of Atoms and Molecules: Theory and Computation* (Springer, New York, 2007).

[20] S. Fritzsche, Phys. Scr., T **100**, 37 (2002).

[21] J. Olsen, M. R. Godefroid, P. Jönsson, P. A. Malmqvist, and C. Froese-Fischer, Phys. Rev. E **52**, 4499 (1995).

[22] P. Jonsson, X. He, C. Froese-Fischer, and I. Grant, Comput. Phys. Commun. **177**, 597 (2007).

[23] C. T. Chantler, J. Phys. Chem. Ref. Data **24**, 71 (1995).

[24] C. T. Chantler, J. Phys. Chem. Ref. Data **29**, 597 (2000).

[25] T. Mukoyama and K. Taniguchi, Phys. Rev. A **36**, 693 (1987).

[26] W. C. Sauder, J. R. Huddle, J. Wilson, and R. E. Lavilla, Phys. Lett. A **63**, 313 (1977).

[27] L. Yin, I. Adler, M. Chen, and B. Crasemann, Phys. Rev. A **7**, 897 (1973).

[28] Y. Ito, T. Tochio, H. Ooohashi, and A. Vlaicu, Radiat. Phys. Chem. **75**, 1534 (2006).